energies

MDPI

Article

Research on High-Frequency Impedance Characteristics of Damaged Circuit Breaker Closing Resistance

Ce Zhang [1], Bo Niu [1], Feiyue Ma [1], Lingjun Yin [2], Shangpeng Sun [1] and Xutao Han [2,*]

[1] Electric Power Research Institute, State Grid Ningxia Electric Power Co., Ltd., Yinchuan 750011, China
[2] School of Electrical Engineering, Xi'an Jiaotong University, Xi'an 710049, China
* Correspondence: xutaohan@xjtu.edu.cn

Abstract

The closing resistor in a circuit breaker are prone to damage during operation due to extreme factors such as over-voltage, over-current, and mechanical shock, which alter their high-frequency impedance characteristics. Comparing impedance before and after damage can indicate the severity of degradation. However, the high-frequency impedance properties of damaged closing resistors remain insufficiently understood. This study investigates three classic damage types through simulation and external testing on a physical circuit breaker, validating the accuracy of the simulation results. Further high-frequency impedance measurements inside the tank examine the characteristics under varying damage degrees. Results show that external testing reflects the intrinsic impedance changes in the resistor string, exhibiting primarily resistive and inductive traits, with negligible capacitive influence. In contrast, internal measurements are affected by the tank's capacitance, leading to a resonance point in the high-frequency range. Different damage degrees cause noticeable shifts in the resonance frequency and a gradual increase in impedance magnitude. These findings offer practical guidance for field inspection of circuit breaker closing resistor conditions using high-frequency impedance techniques.

Keywords: circuit breakers; pre-insertion resistors; high-frequency impedance; damage diagnosis

check for updates

Academic Editor: Mario Marchesoni

Received: 30 September 2025
Revised: 27 October 2025
Accepted: 30 October 2025
Published: 31 October 2025

Citation: Zhang, C.; Niu, B.; Ma, F.; Yin, L.; Sun, S.; Han, X. Research on High-Frequency Impedance Characteristics of Damaged Circuit Breaker Closing Resistance. *Energies* **2025**, *18*, 5768. https://doi.org/10.3390/en18215768

Copyright: © 2025 by the authors. Licensee MDPI, Basel, Switzerland. This article is an open access article distributed under the terms and conditions of the Creative Commons Attribution (CC BY) license (https://creativecommons.org/licenses/by/4.0/).

1. Introduction

Against the backdrop of large-scale application of ultra-high voltage and extra-high voltage power grids, switch-gear such as gas-insulated switch-gear and dead-tank circuit breakers at 750 kV and above voltage levels equipped with closing resistor stacks are widely employed due to their compact structure and high reliability [1–4].

The closing resistor inside the circuit breaker is connected into the circuit via auxiliary contacts prior to the main closing contacts. It utilizes the damping effect of the resistor to suppress electromagnetic oscillations, reduce over-voltage amplitude, and limit the over-voltage generated when energizing unloaded transmission lines. These unique operational characteristics of the closing resistor dictate that during long-term operation, it must withstand extreme mechanical-electrical-thermal coupled stresses such as impact loads from the operating mechanism, over-voltages, and over-currents [5–10]. This easily leads to irreversible failures of the resistor discs, including blackening, charring, cracking, and breakage [11–15], resulting in insulation degradation or the presence of conductive contaminants, which seriously threatens the overall operation of the circuit breaker.

Currently, regarding the damage issues of closing resistors, researchers primarily rely on actual fault cases. Post-fault operation, problems are identified through disassembly inspections, which involve removing all closing resistors for individual examination. Combined with simulation calculations, the causes of equipment failure triggered by closing resistor damage are analyzed and discussed. For instance, Ma et al. uses EMTDC/PSCAD to establish a simulation model, the effect of pre-insertion resistor, pre-insertion resistor insertion duration and closing target angle on closing inrush current and energy absorption by pre-insertion resistor is calculated [16]. Bhatt et al. analyzing the effect of statistical scatter of mechanical operating time (MOT), tolerance of auxiliary contact used as feedback for a controlled switching device, and variation in mechanical insertion time (MIT) and electrical insertion time (EIT) of the PIR-CB [17]. Wang et al. established an impulse current test platform to simulate high-current impact scenarios during switching operations. By applying microsecond-level impulse currents to resistor discs, the time-domain evolution of closing resistance was calculated and analyzed [18].

In recent years research on the detection methods for the damage of closing resistors in circuit breakers has involved multiple fields. Reference [18] utilize ultrasonic sensing to detect the dynamic resistance characteristics of closing resistors. Reference [19] employ wavelet decomposition and the TLS-ESPRIT algorithm to analyze transient and instantaneous current data during the circuit breaker switching process, thereby assessing the operational state of the closing resistor. Although the use of non-contact sensors for detecting closing resistors eliminates the need for switching operations on the circuit breaker and significantly reduces maintenance time, the measurement accuracy remains relatively low.

Although existing research provides some guidance for explaining the causes of circuit breaker equipment failures due to closing resistor damage, it lacks reliable methods for effectively detecting closing resistor damage. Currently, to prevent damaged closing resistors from affecting equipment safety, substations often perform irregular tank-opening inspections on circuit breakers. This approach is highly blind and significantly increases the workload of field equipment operation and maintenance [20–25].

Frequency-sweeping technology has developed rapidly. Ref. [26] proposed a frequency modulation fuze anti-sweeping jamming method based on outlier reconstruction, which utilizes Iterative Filter Decomposition (IFD) and Long Short-Term Memory (LSTM) networks to suppress sweeping jamming. Another application of frequency-sweeping detection technology has been in identifying the coupling error coefficients of micro-electromechanical gyroscopes. This work derived the identification method for coupling error coefficients and analyzed the impact of amplitude and phase detection errors on identification accuracy through numerical simulation [27]. Furthermore, a machine learning-based method for correcting distortions in OCT images has been proposed, demonstrating the use of machine learning techniques to improve the outcomes of frequency-sweeping processes [28].

In theory, when minor microscopic defects occur in the closing resistor, the high-frequency impedance characteristics of the entire resistor stack change. Measuring these changes in high-frequency impedance characteristics could enable diagnostic analysis of its damage condition. However, current domestic attention to high-frequency impedance detection for circuit breaker closing resistors is insufficient. The frequency-sweep impedance method is mostly used in the field of transformer winding deformation detection. Therefore, conducting high-frequency impedance tests on damaged circuit breaker closing resistors and further researching the high-frequency impedance characteristics measured both outside and inside the tank for closing resistors under different damage conditions hold significant practical engineering and scientific research importance.

Based on this, this paper investigates the high-frequency impedance characteristics of closing resistors with varying degrees of damage by leveraging the frequency-sweeping

impedance method, combined with simulation analysis and field tests. In the context of UHV systems, the 800-kV circuit breaker is currently the most prevalent and widely deployed type equipped with a pre-insertion resistor assembly. To address the fault issues caused by damage to the pre-insertion resistors, internal tank detection of the closing resistor is performed on an actual 800 kV circuit breaker to further study the variations in its high-frequency impedance characteristics under such conditions. This approach allows for the identification of damaged closing resistor positions based on their characteristic changes before deciding on removal, thereby shortening maintenance downtime. Approximately three-quarters of the time can be saved in the disassembly step of the pre-insertion resistor string. The study aims to provide reference and guidance for the field application of high-frequency impedance-based detection of closing resistor damage in intact circuit breakers.

2. Simulation Results of the Damaged Closing Resistor

2.1. Simulation Model

Currently, the closing resistors used in power equipment mainly employ Al-Si-C series resistor materials. The constituent phases of Al-Si-C series closing resistors can be categorized into three types: ceramic phase, pores, and graphite. Among these, both the ceramic phase and the pores are insulating phases, while graphite is a conductive phase (semi-metal). Therefore, its electrical equivalent circuit can be represented by a parallel connection of a series resistive-inductive conductive path and a capacitive insulating path.

The closing resistor within the circuit breaker has a series stacked structure. It is assembled on an insulating rod, with compression springs ensuring reliable electrical contact between resistor discs. Both ends are connected via terminal plates in series with metal plates to achieve uniform electrical signal transmission. Thus, when the resistor disc material is homogeneous, each resistor disc can be considered equipotential and equivalently represented as a single RLC circuit in the simulation model. For the entire closing resistor stack, referring to the actual number of resistor discs, it can be viewed as a series connection of numerous identical resistor discs. In the model, this is represented by a series connection of numerous identical RLC circuits. The established equivalent RLC network circuit model is shown in Figure 1.

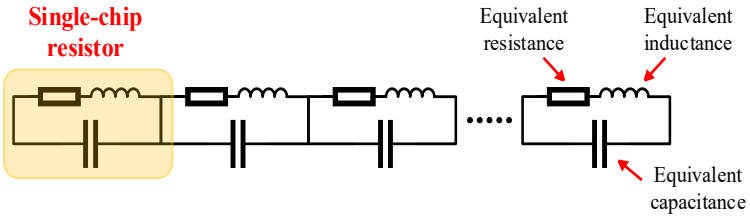

Figure 1. Equivalent circuit model of the closing resistor string.

This paper selects three typical types of damage for simulation: discoloration and charring damage, through-crack damage, and edge breakage damage. Among these, discoloration and charring damage and edge breakage damage only require modifying the parameter values of the equivalent circuit of the damaged resistance sheet according to the actual damage conditions. In contrast, through-crack damage necessitates a change in the circuit topology.

When through-crack damage occurs in the closing resistor, a gas gap forms at the crack location. For simulation, the equivalent circuit topology is altered by representing the RLC circuit shown in Figure 1 as the parallel RLC circuit illustrated in Figure 2. The crack is treated as a medium with the same dielectric constant as the gas inside the circuit breaker tank, and its equivalent capacitance is calculated accordingly.

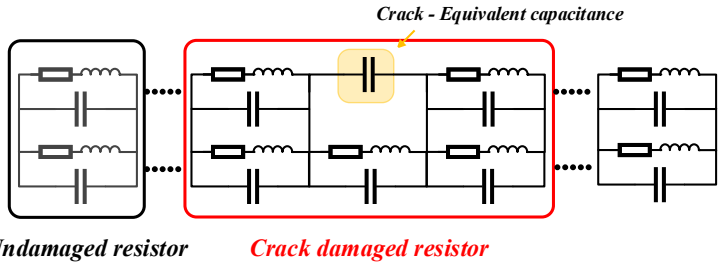

Figure 2. Equivalent circuit model of the crack damaged closing resistor string.

2.2. Edge Drop Damage

Based on the measured variations in the equivalent parameters of the closing resistor string under different damage conditions, as shown in Table 1, the resistance and inductance parameters in the equivalent circuit model illustrated in Figure 1 were modified to reflect the electrical characteristics of the closing resistor under varying degrees of damage.

Table 1. Resistance and inductance values of resistance strings with different degrees of damage.

Degree of Damage	Resistance/Ω	Inductance/μH
Undamaged	156.3	13.30
Minor damage	157.8	13.45
Severe damage	159.3	13.71

Using the previously established simulation model of the closing resistor string, high-frequency impedance tests were conducted on single resistor strings under different damage scenarios. The resulting curves obtained from the simulation results are shown in Figure 3, where the horizontal axis is plotted on a logarithmic scale, S-U represents the comparison between the severely damaged curve and the undamaged curve, while M-U represents the comparison between the mildly damaged curve and the undamaged curve.

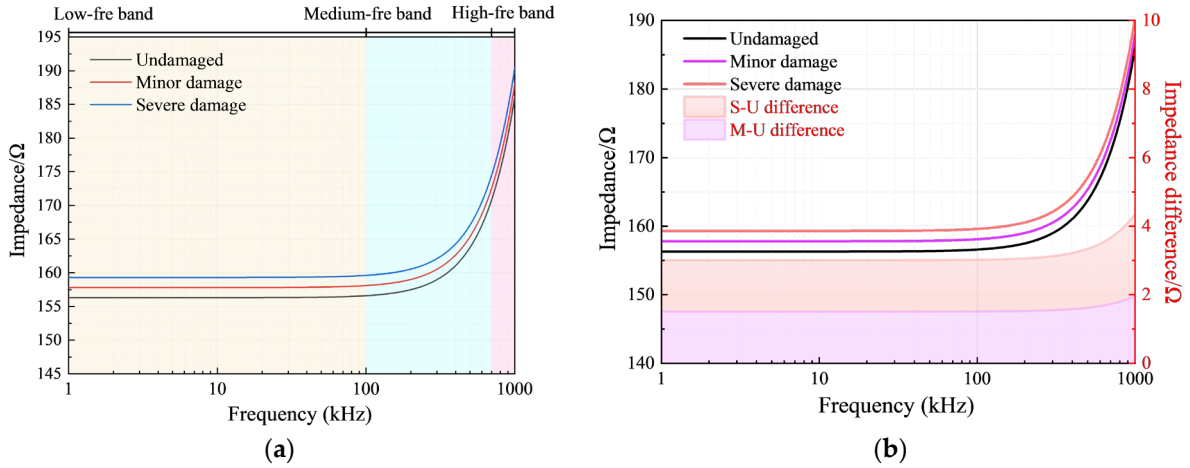

Figure 3. Simulation results of edge drop damage. (**a**) Impedance characteristic curve. (**b**) The difference in impedance curves before and after damage.

As can be seen from the test results in Figure 3, the impedance of the closing resistor string generally exhibits an increasing trend with the rise in the applied frequency, indicating the presence of a significant parasitic inductance effect in addition to its inherent resistive characteristics. Its impedance behaviour shows distinct differences across various frequency bands. In the low-frequency range of 1 kHz to 100 kHz, the inductive effect is not yet pronounced, and the closing resistor string primarily exhibits resistive characteristics, with its impedance value being close to the DC resistance measured directly by

a multi-metre. In the mid-frequency range of 100 kHz to 700 kHz, the parasitic inductance gradually becomes influential, leading to a slow increase in impedance with rising frequency. However, at this stage, the inductive effect remains smaller than the resistive component, so the impedance curve does not show a distinct linear upward trend. In the high-frequency range of 700 kHz to 1 MHz, the inductive effect dominates, and the impedance of the closing resistor string increases approximately linearly with frequency.

For the difference in impedance curves before and after damage, in the low-frequency and mid-frequency bands, it is mainly affected by the change in resistance value, and the difference is almost a straight line. In the high-frequency band, it gradually increases due to the influence of parasitic inductance, and the curve difference shows a gradually increasing trend.

2.3. Entire Crack Damage

The crack damage of the closing resistor reduces the effective cross-sectional area for current flow, increases the path length, and leads to an increase in resistance. At the same time, the cracks damaged the integrity of the resistor sheet, weakened the eddy current cancellation effect, intensified the magnetic flux change, and led to an increase in inductance.

Simulations were conducted on closing resistors with full-section cracks of varying damage degrees, and the obtained high-frequency impedance curves along with their difference comparisons are shown in Figure 4.

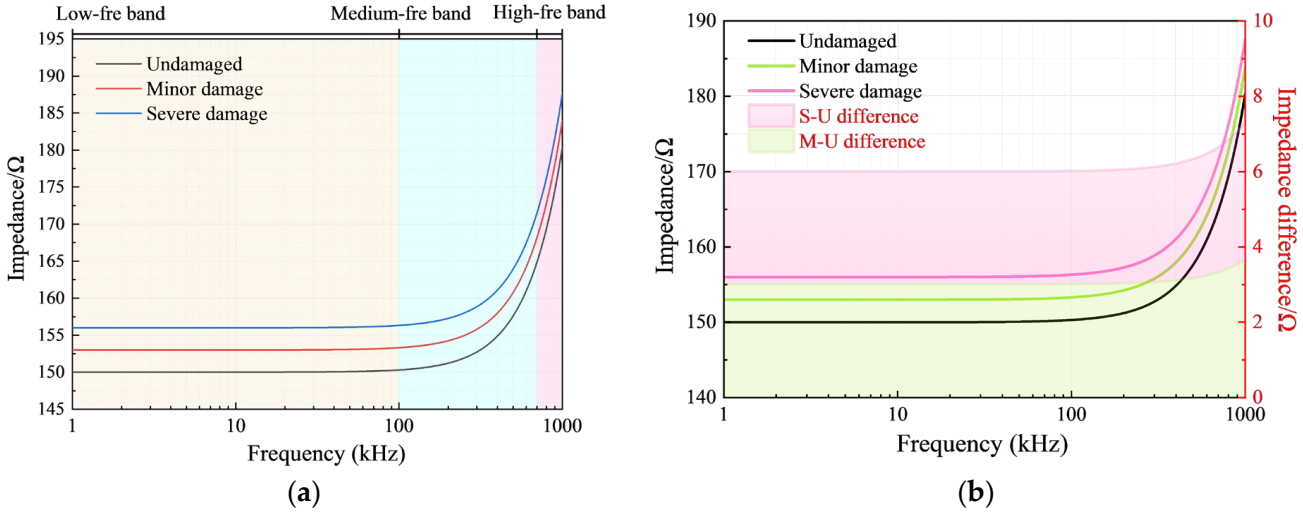

Figure 4. Simulation results of entire crack damage. (**a**) Impedance characteristic curve. (**b**) The difference in impedance curves before and after damage.

The results indicate that the variation trend of the impedance curve under full-section crack damage is similar to that observed in edge loss damage. Notably, the difference in the impedance curve between the damaged and undamaged conditions exhibits a gradual increase only in the high-frequency range.

2.4. Blackened and Charred Damage

When a closing resistor suffers from blackening and charring damage due to factors such as mechanical shock and energy injection, black particles like carbon and metal oxides appear on the material surface. These substances possess significantly lower electrical conductivity than the resistor material, resulting in a permanent and irreversible increase in the resistivity of the resistor string. In severe cases, the material surface may exhibit

bulging and peeling, while the internal structure becomes loose and porous, leading to an overall increase in the inductance of the resistor chip.

Simulations were performed on closing resistors with varying degrees of blackening and charring damage, and the obtained high-frequency impedance curves along with their difference comparisons are shown in Figure 5.

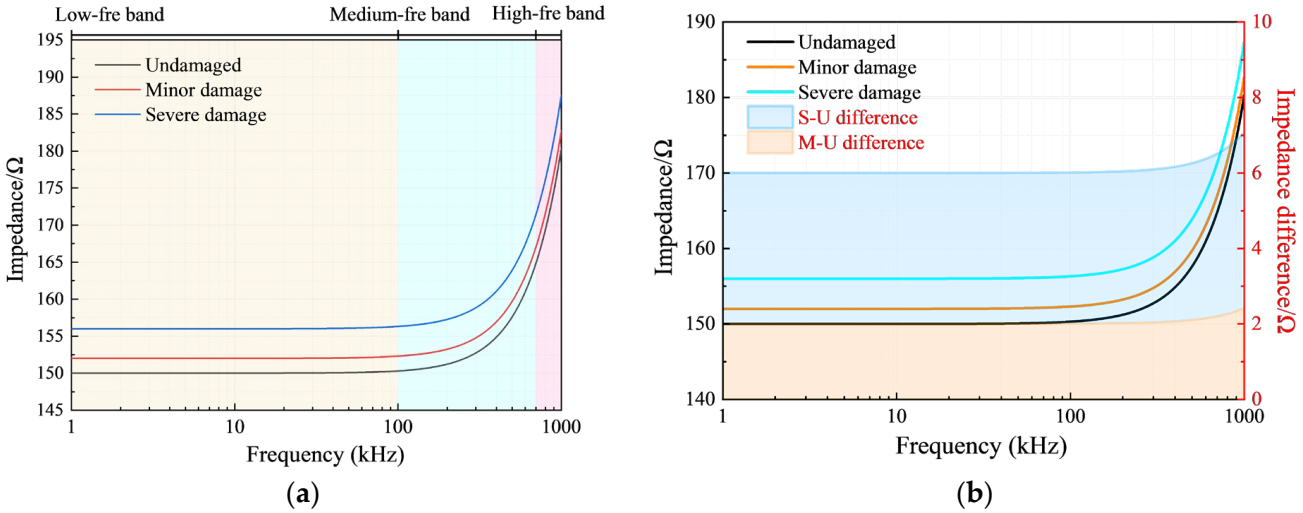

Figure 5. Simulation results of blackened and charred damage. (**a**) Impedance characteristic curve. (**b**) The difference in impedance curves before and after damage.

As can be seen from the figure, the variation trend of the impedance curve and the difference curve before and after damage is almost identical to that of the first two damage types.

For the three aforementioned types of closing resistor damage, the variation trends of the high-frequency impedance curves under different damage levels are generally consistent. In the low-frequency range, the curve approximates a straight line, with the impedance value increasing slightly as the frequency rises. In the mid-frequency range, influenced by parasitic inductance, the curve exhibits a noticeable upward trend, while it shows a linear increase in the high-frequency range. Regarding the difference in curves before and after damage, the variation remains largely constant across the tested frequency band, with only a slight increase observed in the high-frequency region.

It can be concluded that the closing resistor overall exhibits resistive-inductive characteristics, while its inherent capacitance has a negligible effect on its high-frequency impedance properties and can be disregarded.

3. On-Site Test Results of the Damaged Closing Resistor

3.1. Wiring Method for Entity Detection

This paper conducts experiments on an 800 kV circuit breaker with a parallel double-break interrupter unit structure in He Nan, China. As shown in Figure 6, the circuit breaker features a symmetrical layout on both sides, with the interrupting chambers located at each end to ensure electrical and mechanical balance. To improve the transient characteristics during the closing operation, closing resistor stacks are installed on both sides, effectively suppressing switching overvoltages and enhancing operational stability.

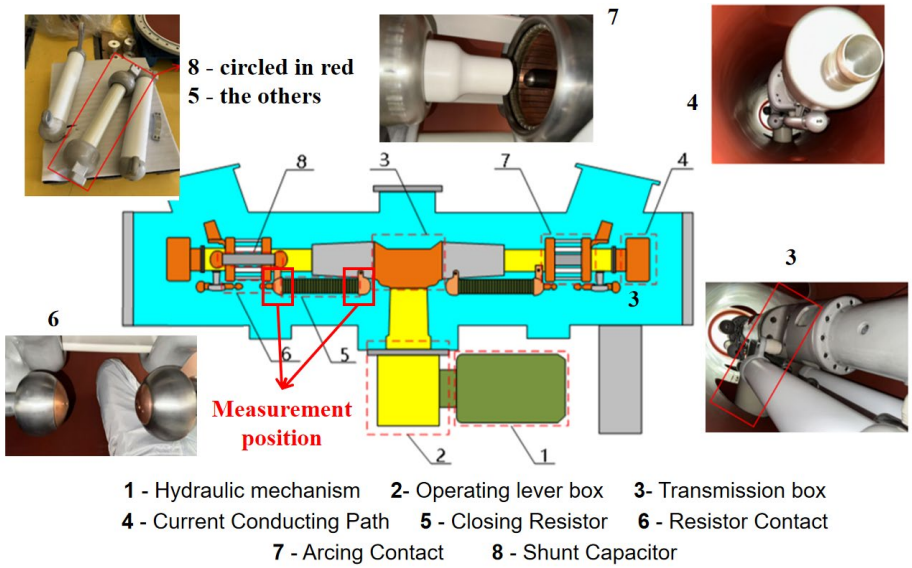

Figure 6. The structure of the test circuit breaker body.

This circuit breaker employs a parallel configuration, and its equivalent circuit is depicted in Figure 7. In the circuit, the closing resistor is connected in series with the auxiliary break and is paralleled with the main break and the grading capacitor to form the complete circuit. Each closing resistor stack consists of 30 resistor discs, with a total resistance of 150 ± 7.5 Ω; the capacitance of the grading capacitor is 700 ± 21 pF.

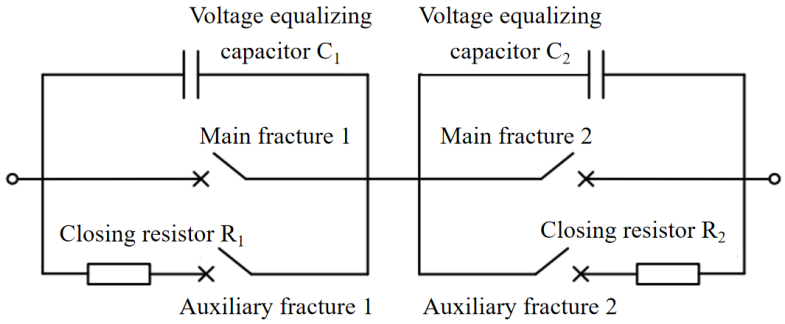

Figure 7. Simplified circuit of the test circuit breaker.

Tests were performed on the closing resistor stacks both outside and inside the tank using a frequency-sweep impedance analyzer to investigate their high-frequency impedance characteristics.

During the testing process, frequent disassembly and replacement of the closing resistors were required. To facilitate operation, the bushings were not installed on the circuit breaker. Consequently, suitable measurement points had to be identified inside the tank for the internal testing.

Resistance measurements were taken at multiple potential locations within the tank using a multimeter. The results indicated that a stable resistance value, approximately 156.7 Ω, was only obtainable at the holes in the insulating rods located in the central area of the circular support bases at both ends of the closing resistor stack. Compared to the nominal resistance of the closing resistor (150 ± 7.5 Ω), the measured value is essentially consistent with the theoretical value. Considering the presence of additional resistance from components such as the aluminum tabs of the resistor discs and the support bases themselves, this result is entirely reasonable within the expected error margin. More importantly, this measurement point provides a reliable conductive path while avoiding

measurement failure caused by the insulating coating, satisfying the requirements from both the physical mechanism and testing feasibility perspectives.

Based on the above factors, this location was ultimately selected as the measurement point for the inside-the-tank tests. When testing a single closing resistor stack inside the tank, the measurement points were chosen at both ends of the stack. The connection method is illustrated in Figure 8.

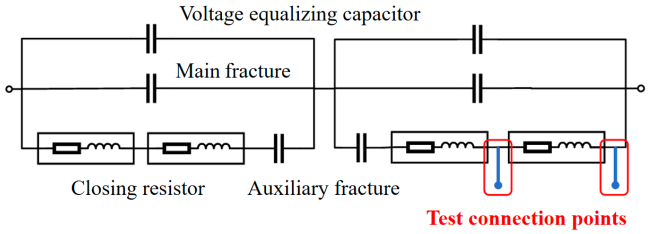

Figure 8. Schematic diagram of the wiring method for closing resistor detection inside the tank.

3.2. Simulation of the Damage Condition of the Closing Resistor

During circuit breaker operation, the most common forms of damage to closing resistors primarily stem from two sources: firstly, the intense mechanical impact generated by opening and closing operations, and secondly, the fragmentation and dislodgment of resistor discs caused by improper assembly. Among these, edge fragmentation, spalling, and subsequent dislodgment of resistor discs represent the most typical and significantly hazardous damage mode. Based on this, this study selects edge fragment loss as the representative damage mode for simulation experiments.

The morphology of the edge fragment loss under different damage severity levels is shown in Figure 9. This study uses the lost volume fraction of the resistor disc as the evaluation metric for damage severity: loss of approximately 1/8 of the volume is defined as slight damage, while loss of approximately 1/4 is defined as severe damage. To more closely simulate actual conditions, small fragments were additionally introduced at the breakage locations on the South and North Non-mechanism-side resistor stacks to simulate fragmentation caused by switching impacts or assembly defects.

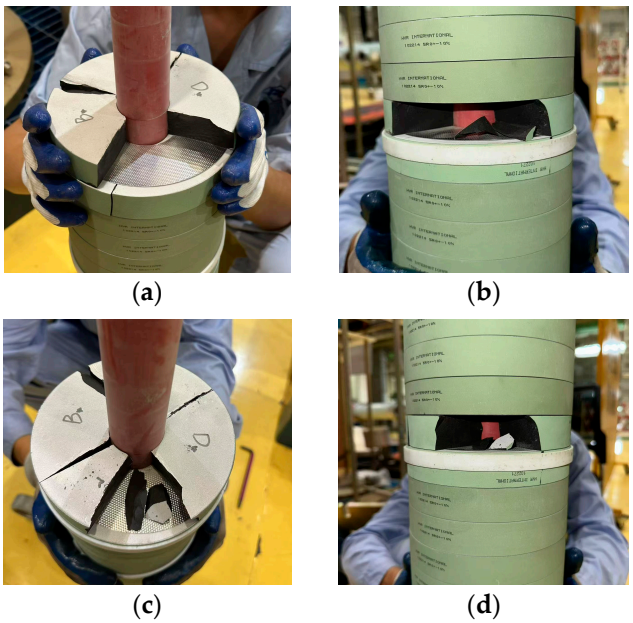

Figure 9. Simulation of closing resistor damage. (**a**) Top view of severely damaged resistance string. (**b**) Front view of a severely damaged resistor string. (**c**) Top view of minimally damaged resistance string. (**d**) Front view of a minimally damaged resistor string.

After assembling the resistor stacks, the overall resistance of the stacks under different damage states was measured using a multi-metre; the results are presented in Table 2. It can be observed that under both slight and severe damage conditions, the overall resistance of the closing resistors exhibited only minor changes. Relying solely on resistance measurement often proves difficult for effectively distinguishing the degree of damage.

Table 2. The measured resistance value of the resistance series.

Degree of Damage	M-South	M-North	N-South	N-North
Undamaged	156.4 Ω	155.6 Ω	156.5 Ω	156.3 Ω
Minor damage	157.7 Ω	157.6 Ω	157.8 Ω	157.8 Ω
Severe damage	158.4 Ω	158.8 Ω	158.6 Ω	159.3 Ω

The test subjects are the four closing resistor stacks inside the circuit breaker. Since the hydraulic mechanism is located on the right side of the breaker, the resistor stacks on the right are designated as the mechanism-side closing resistors, and those on the opposite side as the non-mechanism-side closing resistors. Based on their relative positions, they are specifically named M-south, M-north, N-south, and N-north.

The traditional method for diagnosing closing resistor damage, which relies solely on whether the resistance value change exceeds ±5%, may overlook certain cases where damage is already significant. The frequency-sweeping impedance testing method proposed in this study can, to some extent, address this limitation.

3.3. Test Results of Closing Resistance

Field tests were conducted on single closing resistor strings under different damage conditions using a frequency-sweeping impedance analyzer, and the resulting curves are shown in Figure 10.

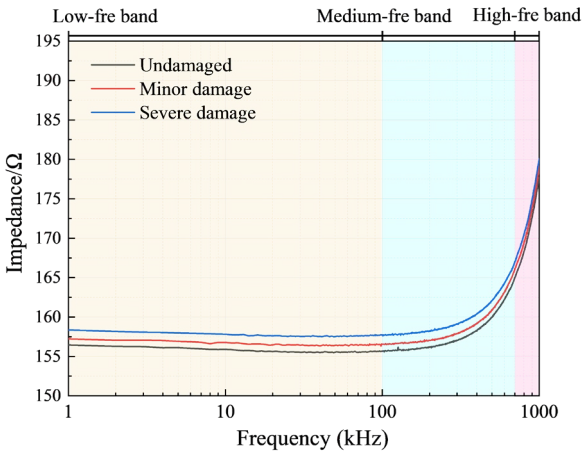

Figure 10. On-site test results.

As can be seen from the figure, resistor strings with different degrees of damage still exhibit resistive-inductive characteristics, meaning the overall impedance of the closing resistor string increases with rising frequency. A comparison of the impedance curves reveals that changes in the degree of damage are primarily manifested in two aspects:

Firstly, in the low-frequency range, the impedance of the closing resistor shows a certain increase as the damage becomes more severe. This is attributed to the reduction in the effective conductive cross-sectional area caused by chipping at the edges of the resistor discs, which narrows the current path and thereby leads to an increase in resistance. Al-

though the magnitude of this change is relatively limited, it still demonstrates a discernible distinction between slight and severe damage.

Secondly, in the high-frequency range, the slope of the impedance curve varies with the degree of damage, reflecting changes in the equivalent inductance of the closing resistor. The underlying reason is that the loss of resistor disc fragments alters the current path and the loop area, resulting in variations in the parasitic inductance. This manifests in the frequency response as differences in the slope of the impedance-frequency curve within the approximately linear region.

The above analysis indicates that the closing resistor string can be electrically modelled as a series combination of a resistor and an inductor. The impedance magnitude of this resistive-inductive element is given by:

$$|Z(j\omega)| = \sqrt{R^2 + (\omega L)^2} \tag{1}$$

where $Z(j\omega)$ is the impedance of the closing resistor string, R is its equivalent resistance, L is its equivalent parasitic inductance, and ω is the angular frequency. Based on Equation (1), the following linear expression can be derived:

$$|Z(j\omega)|^2 = \omega^2 L^2 + R^2 \tag{2}$$

The relationship curve between the square of the impedance and the square of the angular frequency for the closing resistor string, plotted from experimental test data, is shown in Figure 11.

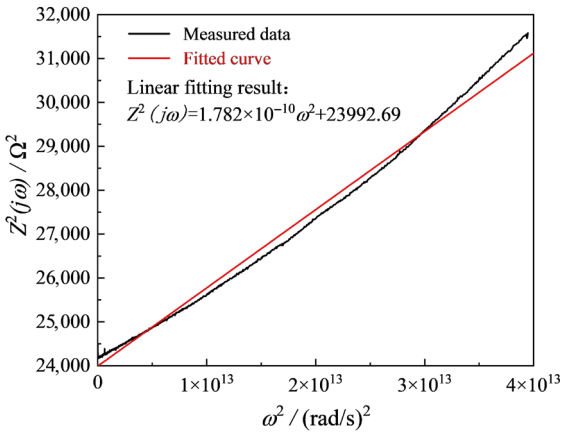

Figure 11. The relationship curve between the square of the string impedance and the square of the angular frequency of a single-string resistor.

The results from Figure 11 confirm that the characteristics of the closing resistor string align with the resistive-inductive model. With a goodness-of-fit greater than 0.999, the fitted equation for the curve is:

$$|Z(j\omega)|^2 = 1.782 \times 10^{-10}\omega^2 + 23992.69 \tag{3}$$

By combining this with Equation (2), the inductance value for the single string of 30 series-connected closing resistors in this study is calculated to be 13.30 μH, and the resistance value is 154.89 Ω. This resistance value is consistent with the result obtained using a multimeter.

Applying the calculation principle of Equation (2), the resistance and inductance values for closing resistor strings with different damage degrees can be obtained, as summarized in Table 3.

Table 3. The resistance and inductance values of resistance strings with different degrees of damage calculated based on the fitting curve results.

Degree of Damage	Resistance/Ω	Inductance/μH
Undamaged	154.89	13.30
Minor damage	155.72	13.42
Severe damage	156.90	13.51

Due to the inherent limitations of the measurement method, imperfect environmental conditions, instrument errors, and other influencing factors, the combined standard uncertainty in the determined resistance parameter $u_{0\Omega}$ is approximately 0.224%, while that for the inductance parameter u_{0L} is approximately 0.447%. The comparison of Tables 2 and 3 indicates that while the resistance values differ slightly, the inductance values are almost identical, which validates the rationality and accuracy of the simulation analysis.

As can be seen from Table 3, after the closing resistor is damaged, both its overall equivalent resistance and inductance increase. Although the change in resistance appears larger in magnitude, this level of variation is often difficult to measure effectively in practical applications. The reasons are twofold: firstly, a 2 Ω increase represents only a minor disturbance relative to the nominal resistance of several hundred ohms; secondly, field testing conditions are complex, where fluctuations in contact resistance and external interference often mask such subtle changes, making damage diagnosis based solely on resistance values unreliable.

In contrast, although the absolute change in inductance (0.2 μH) is relatively small, its effect is significantly amplified in high-frequency testing due to the frequency-sensitive nature of inductance. When the frequency rises to several hundred kHz or higher, the inductive component becomes dominant in the overall impedance, leading to observable differences in the slope of the impedance curve. Compared to low-frequency resistance measurement, this characteristic not only offers better measurability but also exhibits stronger noise immunity under high-frequency conditions. Therefore, the variation in inductance at high frequencies can serve as a more effective indicator for identifying damage in closing resistors. Consequently, establishing a damage diagnosis criterion based on high-frequency impedance characteristics is more feasible and valuable for engineering applications than relying solely on DC or low-frequency resistance measurements.

A comparison between the simulation curve under undamaged conditions and the field test curve, along with the calculated difference between them, is shown in Figure 12.

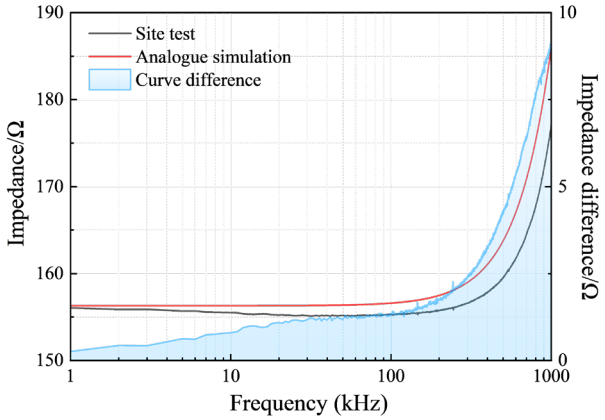

Figure 12. Comparison of simulation results with test results.

As observed in the figure, the discrepancy between the curves is relatively small in the low-frequency range. As the frequency increases, the difference gradually grows, showing

a significant and linearly increasing trend in the mid- and high-frequency ranges, the discrepancy between the curves increases gradually from 0.5% at 1 kHz to 5.6% at 1 MHz. The discrepancy in the low-frequency region is primarily attributed to the difference in resistance values, while the difference in the high-frequency region is mainly influenced by the variation in inductance values. Since the reactance variation is linearly proportional to the frequency, the curve discrepancy exhibits a linear growth trend. Influenced by factors such as inherent measurement errors of the sweep-frequency impedance system (e.g., test cables, clip positioning), structural complexity of the test object, and environmental interference, the field results exhibit a descending trend in the mid-frequency range.

3.4. Test Results of the Closing Resistor in the Tank

The circuit breaker used in this study has two closing resistor stacks arranged on the same side, connected by a link located near the centre of the breaker. In a practical internal tank test, measuring only a single resistor stack would require manual entry into the tank or partial extraction of the internal structure to connect one end of the test circuit directly to this linking piece. This procedure is not only time-consuming and labour-intensive but also increases the uncertainty and operational risk of the experiment. In light of this, for testing damaged closing resistors, this study selected both resistor stacks on the same side as the test subject.

Figure 13 shows the impedance curves obtained from in-tank tests performed on two closing resistor stacks on the same side under different damage conditions. As can be observed from the figure, resonance points appear in the high-frequency band for the impedance curves under all damage conditions. A comparison of these curves reveals that the variation in the degree of damage is reflected across all three frequency bands.

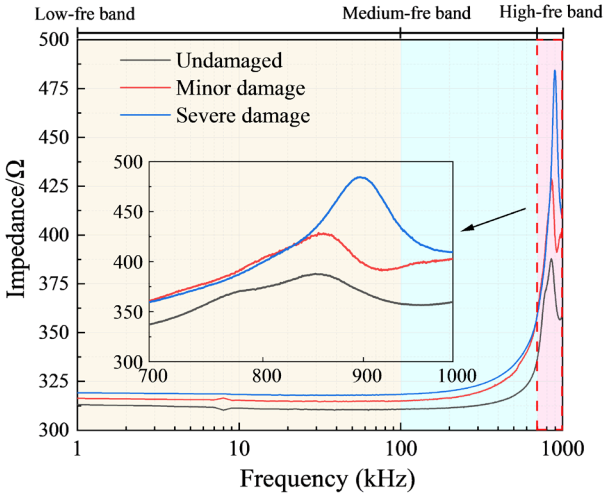

Figure 13. The impedance curves of resistance string inside the tank with different degrees of damage.

Firstly, in the low-frequency band, the change in the impedance value of the closing resistors is consistent with the impedance characteristic changes observed during the out-of-tank tests on a single resistor stack under different damage conditions. As the severity of the damage increases, the impedance shows a certain degree of increase. Furthermore, the magnitude of this change exhibits distinguishable differences between slight and severe damage states.

Secondly, in the medium-frequency band, the rate of rise in the impedance curve varies with the extent of damage. The more severe the damage to the resistor stack, the faster the rise in the curve in this band. The contrast between the curves for damaged and undamaged conditions is more pronounced in the in-tank test compared to the out-of-tank

test. The reason for this is that the capacitive effects of various components within the circuit breaker cause the rising trend, typically observed in the high-frequency band during out-of-tank tests, to manifest earlier.

Finally, in the high-frequency band, significant changes are observed at the resonance points of the impedance curves for different damage levels, with the resonant frequencies and corresponding impedance listed in Table 4. Measured values presented in Table 4 are averaged from five repeated measurements, and the resonance point positions show negligible variation across tests. The impedance at the resonance point of the curve changes with the damage severity; more severe damage results in a higher resonant point impedance.

Table 4. The resonant point of the same side closing resistor string tested in the tank.

Degree of Damage	Undamaged	Minor Damage	Severe Damage
Resonant frequency	869 kHz	854 kHz	897 kHz
Resonant point impedance	421.44 Ω	478.84 Ω	534.39 Ω

The reason for the resonant peak in the impedance curve during the internal tank test is as follows. As shown in Figure 7, when testing a single closing resistor stack inside the breaker, both the main and auxiliary breaks are in the open state, primarily exhibiting capacitive effects. They can be considered as capacitors, similar to the grading capacitor. Therefore, the measurement circuit simplifies to a parallel combination of the single resistor stack and a series circuit of another resistor stack and a capacitor. Since an independent closing resistor stack exhibits resistive-inductive characteristics, the introduction of capacitance into the loop creates a resonant frequency point.

These results indicate that when detecting closing resistors inside the circuit breaker tank, the influence of damage-induced inductance changes on the high-frequency impedance characteristics is amplified. The frequency range where the inductive component dominates the impedance shifts towards lower frequencies. The distinguishing feature of the curves evolves from a change in slope in the out-of-tank test to a more pronounced and easily identifiable shift in the resonance point in the in-tank test. This provides stronger evidence supporting the use of inductance variation characteristics at high frequencies as an effective indicator for assessing the damage state of closing resistors.

Based on the changing trends of the sweep frequency curves of the closing resistors with different damage degrees obtained from the above image, we have summarized a set of damage assessment standards for circuit breaker closing resistors for subsequent reference. This standard is defined by three judgement criteria: Initial value change ratio r, Resonance point frequency shift ratio r_1, Resonance point impedance shift ratio r_2.

The average value a of the low-frequency band is calculated from N1 data points. This value is then compared with the baseline average b obtained under undamaged conditions to determine the initial value shift ratio of the curve $r = |a - b|/b$. This ratio serves as an indicator for assessing the extent of closing resistor degradation.

Furthermore, the resonant frequency f and its corresponding impedance Z at the resonance point within the high-frequency band are identified. These parameters are compared with their baseline counterparts, the resonant frequency f_0 and impedance Z_0 from the undamaged state, to calculate the frequency shift ratio r_1 and the impedance shift ratio r_2 at the resonance point, where $r_1 = |f - f_0|/f_0$ and $r_2 = |Z - Z_0|/Z_0$. The degradation level of the closing resistor is subsequently evaluated based on these calculated ratios. The extent of degradation can be determined upon the fulfilment of any one of these specified ratio-based criteria. The specific criteria for judgement corresponding to different degrees of injury are shown in Table 5.

Table 5. The basis for judging the degree of damage to the closing resistor.

Degree of Damage	Resonance Point Shift Ratio r_1, r_2 Initial Value Change Ratio r
Severe damage	$r_1 \geq 5\%$ or $r_2 \geq 20\%$ or $r \geq 15\%$
Moderate damage	$2\% \leq r_1 \leq 5\%$ or $10\% \leq r_2 \leq 20\%$ or $10\% \leq r \leq 15\%$
Minor damage	$1\% \leq r_1 \leq 2\%$ or $5\% \leq r_2 \leq 10\%$ or $7.5\% \leq r \leq 10\%$
Undamaged	$r_1 \leq 1\%$ and $r_2 \leq 5\%$ and $r \leq 7.5\%$

4. Conclusions

This study employs the frequency-sweep impedance testing method to conduct simulation analysis and field tests on the high-frequency impedance characteristics of closing resistors in real tank-type circuit breakers. The main conclusions are as follows:

(1) For the three classical damage types of the closing resistor, the variation trends of the curves under different damage degrees and the trends in the impedance differences before and after damage are fundamentally consistent, with all cases exhibiting overall resistive and inductive characteristics. When damage occurs, both the equivalent resistance and inductance increase, further demonstrating that the more severe the damage, the more significant the increase.

(2) The frequency-impedance curve obtained from measurements performed on the closing resistor assembly inside the tank exhibits resistive characteristics in the low-frequency segment and reactive characteristics in the high-frequency segment. Moreover, variations in the inductance properties of the closing resistor caused by different degrees of damage demonstrate superior sensitivity and significance compared to changes in resistance. Therefore, inductive characteristics can serve as an effective indicator for identifying the damage state of closing resistors, providing an experimental basis and methodological support for reliable damage detection in subsequent research.

(3) Based on the variation patterns observed in the sweep-frequency impedance curve, we have developed a foundational approach for establishing a standard to diagnose the degradation level of closing resistors using the sweep-frequency impedance method. This approach is based on a combined assessment of the mean value shift in the low-frequency band, and the resonance point shift in the high-frequency band.

The sweep-frequency impedance method employed in this study has contributed to reduced maintenance time and improved detection accuracy for circuit breakers. In future developments of this technique, the trends in frequency-impedance curve variations under different degradation levels summarized in this paper can be leveraged. By incorporating approaches such as machine learning, it would be possible to predict the degradation of closing resistors and further optimize the proposed method.

Author Contributions: Conceptualization, S.S. and X.H.; Methodology, C.Z., B.N. and X.H.; Software, C.Z.; Validation, C.Z. and L.Y.; Formal analysis, B.N.; Investigation, B.N.; Resources, F.M. and X.H.; Data curation, B.N., F.M. and X.H.; Writing—original draft, L.Y.; Writing—review & editing, C.Z.; Visualization, F.M. and L.Y.; Supervision, F.M. and S.S.; Project administration, X.H.; Funding acquisition, S.S. All authors have read and agreed to the published version of the manuscript.

Funding: This research was funded by Science and Technology Project of State Grid Ningxia Electric Power Co., Ltd., grant No. 5229DK24000S.

Data Availability Statement: The original contributions presented in this study are included in the article. Further inquiries can be directed to the corresponding author.

Conflicts of Interest: The authors declare that this study received funding from Electric Power Research Institute, State Grid Ningxia Electric Power Co., Ltd., Yinchuan 750011, China. The funder had the following involvement with the study: Ce Zhang, Bo Niu, Feiyue Ma, Shangpeng Sun.

References

1. Niu, B.; Ma, F.; Xiang, Z.; Wu, H.; Sun, S.; Wen, Q. Research on operation reliability and fault diagnosis technology of pre-insertion resistors for circuit breakers. *Ningxia Electr. Power* **2021**, *1*, 23–35.
2. Legate, A.C.; Brunke, J.H.; Ray, J.J. Elimination of closing resistors on EHV circuit breakers. *IEEE Trans. Power Deliv.* **1988**, *3*, 223–231. [CrossRef]
3. Huang, H.; Li, W.; Lu, W.; Zhang, C.; Chen, W.; Zhou, H. Simulation of radial breakdowns on the breaker grading capacitor of 500 kV AC filter. *High Volt. Appar.* **2018**, *54*, 56–62.
4. Ji, R.; Yi, Q.; Su, F.; Sun, K.; Chen, J.; Zhou, H. Study on applicability of circuit breaker closing resistance in EHV and UHV AC systems. *Power Syst. Technol.* **2011**, *35*, 18–25.
5. Chen, X.; He, C.; Deng, J.; Zhu, X.; Zhang, G.; Ni, H.; Ma, F.; Chen, L. Energization transient suppression of 750 kV AC filters using a pre-insertion resistor circuit breaker with a controlled switching device. *IEEE Trans. Power Deliv.* **2022**, *37*, 3381–3390.
6. Awad, E.A.; Badran, E.A.; Youssef, F.M.H. Mitigation of temporary over-voltages in weak grids connected to DFIG-based wind farms. *J. Electr. Syst.* **2014**, *10*, 431–444.
7. Sun, Q.; Tu, Y.; Fu, J.; Wang, X.; Liu, X.; Zhou, J. Fracture analysis of fastening bolt of closing resistance for 1100 kV GIS circuit breaker. *Zhejiang Electr. Power* **2023**, *42*, 68–74.
8. Shu, S.; Ruan, J.; Huang, D.; Wu, G.; Liu, B.; Zhang, K. Dynamic voltage-sharing measures for vacuum circuit breakers with triple breaks. *Power Syst. Technol.* **2012**, *36*, 252–259.
9. Liu, S.; Lv, D.; Zhang, F. Study on the suppression efficacy of filter closing inrush currents by shunt dynamic closing resistor of circuit breaker. *Power Syst. Technol.* **2024**, *48*, 3931–3937.
10. Yang, R.; Zhang, H.; Zhang, G.; Liu, K.; Wang, Y.; Gao, L. Adaptability of cancellation of the closing resistance of circuit breaker for 330 kV transmission line. *Insul. Surge Arresters* **2023**, *6*, 165–171.
11. Kumar, R.; Bhargava, P. Fabrication of low specific resistance ceramic carbon composites by colloidal processing using glucose assoluble carbon source. *Bull. Mater. Sci.* **2017**, *40*, 1197–1202. [CrossRef]
12. Chen, L.; Chen, X.; Wei, Y.; Wu, C.; Deng, J.; Ma, F. Study of controlled switching with pre-insertion resistor during energization of AC filters. In Proceedings of the 22nd International Symposium on High Voltage Engineering (ISH 2021), Hybrid Conference, Xi'an, China, 21–26 November 2021; pp. 1682–1687.
13. Lazimov, T.; Saafan, E.A.; Babayeva, N. Transitional processes at switching-off capacitor banks by circuit-breakers with pre-insertion resistors. In Proceedings of the 2015 Modern Electric Power Systems (MEPS), Wroclaw, Poland, 6–9 July 2015; pp. 1–4.
14. Hedman, D.E.; Johnson, I.B.; Titus, C.H.; Wilson, D.D. Switching of Extra-High-Voltage Circuits II-Surge Reduction with Circuit-Breaker Resistors. *IEEE Trans. Power Appar. Syst.* **1964**, *83*, 1196–1205. [CrossRef]
15. Niu, B.; Chen, L.; Wu, X.; Ni, H.; Zhang, Q.; Wei, Y. Fault analysis of pre-insertion resistors for circuit breakers used in 750kV ACF. In Proceedings of the 16th IET International Conference on AC and DC Power Transmission (ACDC 2020), Online Conference, 2–3 July 2020; pp. 283–289.
16. Ma, F.; He, C.; Chen, X.; Zhu, X.; Deng, J.; Ni, H. Suppression Methods of 750 kV AC Filter Switching Inrush Surge for Circuit Breakers Having Pre-insertion Resistors. In Proceedings of the 2020 4th International Conference on HVDC (HVDC), Xi'an, China, 6–9 November 2020; pp. 1207–1212.
17. Bhatt, K.A.; Bhalja, B.R.; Parikh, U.B. Evaluation of controlled energisation of an unloaded power transformer for minimizing the level of inrush current and transient voltage distortion using PIR-CBs. *IET Gener. Transm. Distrib.* **2018**, *12*, 2788–2798. [CrossRef]
18. Wang, X.; Chen, Z.; Wu, Y.; Bao, Y.; Wu, X.; Qiu, Z.; Li, S.; Guo, L. Study on the Dynamic Resistance Characteristic of Circuit Breaker Closing Resistor Under Impulse Current. In Proceedings of the 2025 7th International Conference on Energy Systems and Electrical Power (ICESEP), Wuhan, China, 20–22 June 2025; pp. 1206–1211.
19. Ma, F.; Li, A.; Niu, B.; Ni, H.; Liu, B.; Deng, J. Extra/Ultra High Voltage AC Filter Circuit Breaker Pre-Insertion Resistors State Evaluation Based on Wavelet Decomposition and TLS-ESPRIT. In Proceedings of the 2024 4th International Conference on Energy Engineering and Power Systems (EEPS), Hangzhou, China, 9–11 August 2024; pp. 1016–1019.
20. Wu, D.; Zhou, Y.; Li, W.; Li, H.; Xu, Y.; Xia, H. Analysis on a fault of grading capacitor for 500 kV circuit breaker. *High Volt. Appar.* **2016**, *52*, 195–199.
21. Patcharoen, T.; Ngaopitakkul, A. Transient inrush current detection and classification in 230 kV shunt capacitor bank switching under various transient-mitigation methods based on discrete wavelet transform. *IET Gener. Transm. Distrib.* **2018**, *12*, 3718–3725. [CrossRef]
22. Meng, W.; Yin, F.; Chang, Y.; Tang, W.; Wei, J. Research of closing resistor in 800 kV SF6 tank circuit breaker. *High Volt. Appar.* **2020**, *56*, 109–113.

23. Han, B.; Chen, W.; Chen, X.; Ban, L.; Xiang, Z.; Ge, D. Study on Eliminating Closing Resistor of Circuit Breaker by Using Controllable Surge Arrester in UHV System. In Proceedings of the 2018 International Conference on Power System Technology (POWERCON), Guangzhou, China, 6–8 November 2018; pp. 2839–2844.
24. Sun, J.; Dai, H.; Chen, W.; Cui, B.; Yang, F.; Yao, X. Energy Tolerance and Failure Characteristics of Carbon-ceramic Closing Resistor for Circuit Breaker. *High Volt. Eng.* **2024**, *50*, 2590–2600.
25. Liu, K.; Wen, D.; Bao, Y.; Qiu, Z.; Li, S.; Ji, S. Stress distribution numerical simulation and influencing factor analysis of stress under operating shock of pre-insertion resistor of 750 kV dead tank circuit breaker. *High Volt. Appar.* **2023**, *59*, 180–185.
26. Duan, L.; Hao, X.; Chen, Q. Anti-sweep jamming method for FM fuze based on outlier reconstruction. *J. Beijing Univ. Aeronaut. Astronaut.* **2025**, *51*, 1377–1384.
27. Zheng, X.; Xia, C.; Wang, X.; Tong, W. Coupling error coefficient identification based on swept-frequency measurement in MEMS gyroscopes. *J. Chin. Inert. Technol.* **2024**, *32*, 170–179.
28. Ma, C.; Chen, P.; Yang, L.; Han, T.; Tang, Y.; Chen, C.; Ding, Z. A machine learning approach to correct imaging distortions in swept-source optical coherence tomography. *Acta Phys. Sin.* **2025**, *74*, 120–129. [CrossRef]

Disclaimer/Publisher's Note: The statements, opinions and data contained in all publications are solely those of the individual author(s) and contributor(s) and not of MDPI and/or the editor(s). MDPI and/or the editor(s) disclaim responsibility for any injury to people or property resulting from any ideas, methods, instructions or products referred to in the content.